Eur Spine J
DOI 10.1007/s00586-014-3705-0

ORIGINAL ARTICLE

In vivo compatibility of Dynesys® spinal implants: a case series of five retrieved periprosthetic tissue samples and corresponding implants

M. Neukamp · C. Roeder · S. Y. Veruva · D. W. MacDonald · S. M. Kurtz · M. J. Steinbeck

Received: 3 July 2014 / Revised: 24 November 2014 / Accepted: 26 November 2014

Abstract
Purpose To determine whether particulate debris is present in periprosthetic tissue from revised Dynesys® devices, and if present, elicits a biological tissue reaction.
Methods Five Dynesys® dynamic stabilization systems consisting of pedicle screws (Ti alloy), polycarbonate-urethane (PCU) spacers and a polyethylene-terephthalate (PET) cord were explanted for pain and screw loosening after a mean of 2.86 years (1.9–5.3 years). Optical microscopy and scanning electron microscopy were used to evaluate wear, deformation and surface damage, and attenuated total reflectance Fourier transform infrared spectroscopy to assess surface chemical composition of the spacers. Periprosthetic tissue morphology and wear debris were determined using light microscopy, and PCU and PET wear debris by polarized light microscopy.
Results All implants had surface damage on the PCU spacers consistent with scratches and plastic deformation; 3 of 5 exhibited abrasive wear zones. In addition to fraying of the outer fibers of the PET cords in five implants, one case also evidenced cord fracture. The pedicle screws were unremarkable. Patient periprosthetic tissues around the three implants with visible PCU damage contained wear debris and a corresponding macrophage infiltration. For the patient revised for cord fracture, the tissues also contained large wear particles (>10 μm) and giant cells. Tissues from the other two patients showed comparable morphologies consisting of dense fibrous tissue with no inflammation or wear debris.
Conclusions This is the first study to evaluate wear accumulation and local tissue responses for explanted Dynesys® devices. Polymer wear debris and an associated foreign-body macrophage response were observed in three of five cases.

Keywords Dynesys® · Implant wear · Deformation · Wear debris · Inflammation

M. Neukamp · C. Roeder
Institute for Evaluative Research in Medicine, University of Bern, Bern, Switzerland

S. Y. Veruva · D. W. MacDonald · S. M. Kurtz · M. J. Steinbeck (✉)
Implant Research Center, School of Biomedical Engineering, Science, and Health Systems, Drexel University, 3401 Market St, Suite 345, Philadelphia, PA 19104, USA
e-mail: mjs348@drexel.edu

S. M. Kurtz
Exponent Inc., 3440 Market St. Suite 600, Philadelphia, PA 19104, USA

M. J. Steinbeck
Department of Orthopaedic Surgery, Drexel University College of Medicine, 245 N. 15th Street, Philadelphia, PA 19102, USA

Introduction

The Dynesys® (Zimmer® Spine, Minneapolis, MN) implant was developed as a posterior dynamic stabilization system in an attempt to overcome the disadvantages of fusion in the treatment of degenerative disorders of the lumbar spine [1]. Its design was based on the premise that restoring or maintaining the normal biomechanical function of the spine is better than eliminating segmental motion and the consequent negative effects on the adjacent segments. This system consists of titanium (Ti) alloy (Protasul® 100) pedicle screws, a spacer made of polycarbonate urethane (Sulene®-PCU) and a cord made of polyethylene-terephthalate (Sulene®-PET). The PET cord connects the pedicle screws and runs through the hollow

Published online: 06 December 2014

core of the PCU spacers, which fits between the pedicle screw heads. The PET cord limits flexion, whilst the PCU spacer keeps the vertebrae in an upright position and limits the extension of the spine.

Several clinical studies have evaluated the safety and effectiveness of this device. The clinical outcome showed significant improvement regarding pain, function and disability scores [2–5]; however, the treatment indications varied and so comparison of the results was difficult [6]. One noteworthy finding was that for patients with a clear indication of degenerative spondylolisthesis, progression was prevented within the first 4 years [3, 7]. Compared to fusion surgery, Dynesys® provided comparably good outcomes in these patients, leading to the assumption that the Dynesys® stabilization system was as safe and effective as a fusion procedure [3, 5]. However, for patients initially diagnosed with degenerative disease (disc/stenosis) associated with instability, lumbar pain and overall function scores did not consistently reflect a clinically relevant improvement after surgery [8, 9]. Both studies reported that 19 % required or were scheduled for a further surgical intervention within the first 2 years. Other investigations have also shown a progression of adjacent segment degeneration [3, 7, 10]. Thus, no definitive conclusions can be drawn until long-term data are made available for the device. The overall number of complications requiring revision of Dynesys® reported in the literature ranges from 19 to 34 % [5, 8, 9, 11–13], with screw loosening being the typical problem (rates vary from 3.2 to 21 %) [4, 7, 11, 12, 14]. However, similar to posterior fusion techniques, this procedure eliminates the complications and morbidity of harvesting bone grafts for interbody fusion.

The Dynesys® system was developed with the theoretical biomechanical end goal of achieving functional spinal unit stability, while allowing physiologic motion. During this motion, the PCU spacers bear the bulk of compressive loads, while the PET cords bear tensile loads. Biomechanical effects of the Dynesys® stabilization system in comparison to other posterior dynamic systems, a rigid posterior stabilization rod system and the native situation were evaluated by Schilling et al. [15] in lumbar cadaver specimens. Analysis in flexion, extension and lateral bending revealed the Dynesys® system, instrumented at the L4–L5 level, significantly reduced the range of motion (ROM) and neutral zone compared to the native situation of functional spinal units; there was no difference when compared to the rigid fixation device. However, during axial rotation, the dynamic system maintained ROM at the level of the native intersegmental rotation. Similarly, other cadaveric studies found the implant stabilized the specimens in flexion–extension and lateral bending, but failed to significantly limit motion in axial rotation or torsion [16, 17]. Taken together, the current literature suggests that dynamic stabilization systems can permit controlled movements as an advantage over rigid fixation during flexion/extension and bending, but there is concern that the Dynesys® does not provide stabilization during intersegmental rotation which may ultimately affect the performance of these devices.

Published Dynesys® retrieval analyses describe surface damages such as scratches, imprints of contact with pedicle screws or PET cord, plastic deformations to the PCU spacer and fraying of the outer fibers of the PET cords [18–20]. The biostability and in vivo degradation of the PCU spacer and PET cord were analyzed in these studies using attenuated total reflectance Fourier transform infrared spectroscopy (ATR-FTIR) and gel permeation chromatography. For the PET cords, no signs of hydrolytic degradation or changes in the molecular weight could be verified, and the PCU spacers showed only small changes in the surface chemistry at longer implantation times [19], suggesting good short-term biostability.

These inconsistencies make it difficult to determine the overall safety of the Dynesys® implant as an alternative to fusion, thereby mandating a need for further investigations on wear-related damage in vivo and its associated biological responses. The aim of the current study was to evaluate the in vivo performance of five Dynesys® retrievals, revised after a mean of 2.86 years (1.9–5.3 years) for pain and screw loosening, by determining the presence of polymer wear debris in the context of local tissue reactions in periprosthetic tissues.

Materials and methods

Implant, tissue collection and patient clinical information

Five Dynesys® lumbar spinal implants and corresponding tissue samples taken from around each implant were obtained at the time of revision surgery. All surgeries and tissue specimen retrievals were performed at two surgical centers in collaboration with an urban biomedical engineering department. Tissues were de-identified and collected in accordance with an IRB-approved protocol. All tissue and implant analyses were performed following the ASTM standard F561: standard practice for retrieval and analysis of medical devices, and associated tissues and fluids. The radiographs and operative notes were reviewed in all cases. An overview of the clinical information is provided in Table 1.

Table 1 Clinical information for Dynesys® cases at index and revision surgery

Case	Gender	Age at Dynesys® insertion	Primary diagnosis	Implantation time years	Surgical site of revision surgery	Revision reason	Revision surgery	Incidental findings after revision surgery
DYN 005	F	49	Disc degeneration L3/4, L4/5, L5/S1	2.5	L3–L4	Recurring back pain	Only level/part L3/4 of the Dynesys® fixation was removed	Screw loosening (L3), fibrosis around Dynesys® system
DYN 006	F	48	Disc degeneration L5/S1	1.9	L5–S1	Persistent low back pain and pain in left and right leg	Postero-lateral fusion in situ with iliac crest bone	Loose S1 screws with neural irritation; fibrosis
DYN 009	F	44	Disc degeneration L4/5 L5/S1, hyperlordosis	2.4	L4–L5, L5–S1	Persisting pain after a short pain relief	Implant removal, no fusion	Loose screws in L4 and S1
DYN 015	M	47	Pseudarthrosis of previous fusion at L5/S1, disc herniation and spinal stenosis at L4/5	2.2	L3–L4, L4–L5	Pain	Non-instrumented postero-lateral fusion	Loosening of screws L3 bilaterally and L5 left
BRSP011	M	54	Disc degeneration, discogenic pain	5.3	L3/4L5/S1	Pain, osteolysis	Dynesys® implants removed	"Disrupted" cord bilaterally (left L3/4, right L4/5), loose screws L3 left and S1 bilaterally

Implant analysis for wear, surface damage, and spacer chemical changes

Four of the implants were from an implant retrieval series previously analyzed for wear, surface damage and chemical properties by Ianuzzi et al. [19]. Surfaces were first examined optically under a stereomicroscope with a Leica camera (Type DFC 490, Leica Microsystems, Switzerland) to assess surface damage, gross fracture and mechanisms such as scratching, abrasion, material cracking, delamination and plastic deformation. PCU spacers were evaluated to determine the extent of plastic deformation along the length. The cord components were examined for the evidence of contact with the spacer, pedicle screw or set screw. Regions with macroscopic alterations were further analyzed by scanning electron microscopy (SEM; JSM-639OLV, JEOL, Japan). To study changes in chemical structure at the surfaces of retrieved and exemplar (never-implanted) PCU spacers, on the cut and molded ends, as well as along the length, the spacers were evaluated using ATR-FTIR (Thermo Electron Corp., Waltham, MA). Spectra were recorded with a diamond crystal, averaging 64 scans per spectrum, and analyzed using Omnic 7.1a (Thermo Electron Corp.). Regions of interest included the carbonyl stretch between 1,650 and 1,800 cm^{-1}, associated with morphological rearrangement and phase separation of the hard and soft segment microdomains, as well as the presence of peaks at 1,174 and 1,650 cm^{-1}, associated with ether branching and free aromatic amines; both, indicative of biologic oxidative degradation of PCU [21].

Tissue analysis

Tissues collected from revision surgeries were fixed in 10 % formalin and bone was avoided based on microCT imaging (μCT 80, Scanco Medical, Brüttisellen, Switzerland) of the tissue. Two representative 4-mm punches from each surrounding soft tissue were embedded in paraffin blocks. Serial 6-μm sections were procured, de-waxed and stained with Alcian blue (Electron Microscopy Sciences, Hatfield, PA) hematoxylin, and eosin (H&E) (ThermoFisher Scientific, Waltham, MA). Entire tissue sections were imaged (typically 16 fields) under transmitted light microscopy at 100× (10 objective) using a Motic BA300POL microscope (Motic, Richmond, British Columbia, Canada), equipped with a stepper motor-controlled stage and ProgRes SpeedXT core 5 (Jenoptik, Jena, Germany) microscope camera.

Tissues were scored using the Oxford-ALVAL scoring system [22, 23] for inflammation resulting from macrophage infiltration and necrosis (Table 2). We also used a similar semi-quantitative score for lymphocyte infiltration and the degree of tissue vascularization as summarized in Table 2. The presence of cartilage was determined using alcian blue stain, and reported if present. Tissues were independently scored by two observers and the results agreed within 90 %.

Wear debris analysis

PCU and PET particle number, size, and shape were determined using 200X polarized light images [24] according to the ASTM Standard Practice for Characterization of Particles. In brief, images were analyzed using a customized image threshold operations programmed in Matlab^{TM} (Mathworks, Inc., Natick, MA) and a customized macro in NIH ImageJ (National Institutes of Health, Bethesda, MD) was applied to each image to determine wear particle characteristics. The resulting particle number was then converted into number per mm^2 area of tissue using a measured conversion factor of 0.295 μm/pixel. All images were visually reviewed to ensure that false positive signals from birefringent collagen did not contribute to particle analysis results.

Results

Implant analysis

Macroscopic and microscopic observations revealed that all explanted devices exhibited signs of surface damage (Table 3). While commonly observed abrasive scratches on the PCU spacers were mostly attributed to iatrogenic damage, spacers from 3 of 5 devices exhibited abrasive wear zones, likely from impingement with surrounding bony structures. Plastic bending deformation was observed in all spacers, ranging from 0.2° to 13.6° (mean 2.9°); however, only two systems had spacers that were deformed greater than 5°. Plastic deformation was also evident on the surfaces where the PET cord exited the spacer (not shown). All five devices showed evidence of imprints from the articulating pedicle screw and PET cord (Fig. 1). The PET cords showed fraying of the outer fibers in all implants, likely from abrasion with surrounding component (Fig. 2a, b). In addition to fraying, the cord from BRSP 011 was fractured; images of the left side implant cord fracture, disrupted ends and an SEM image of the cross sections of the disrupted end are shown in Fig. 2c, d). Other surface damage included scalpel scratches on pedicle screws from surgical removal, but none of the screws exhibited signs of damage from bony fixation or ingrowth.

ATR-FTIR results showed a new absorption peak at 1,650 cm^{-1} in spacers from 1 of 5 devices (Fig. 3) when compared against exemplar spacers. The altered absorption in spacers from BRSP 011 is indicative of a change in the phenyl signal, which suggests oxidative biodegradation involving the urethane segment [25]. Additionally, inconsistent intensities of the H-bonded and free carbonyl signals in the carbonyl stretch were also noted, suggestive of altered morphological organization and composition. Interestingly, the BRSP 011 implant had the longest implantation time of 5.3 years.

Tissue analysis

Table 4 provides an overview of the tissue analysis results for all five cases. Tissue morphologies were similar in patients without wear. Three of the patient tissues contained wear debris and an associated macrophage infiltration. For cases DYN 006 and DYN 015, which displayed abrasive wear zones on the spacers, phagocytosable wear debris (0.15–10 μm) and inflammation were observed in 1 of 3 and 3 of 4 periprosthetic tissues, respectively (Fig. 4). In the case with the disrupted PET cord (BRSP 011) and spacer damage, all of the collected tissues contained wear debris of varying sizes (Fig. 5). Within these tissues were regions with extensive inflammation consisting of macrophages and giant cells in direct association with both phagocytosable and large wear debris (>10 μm), respectively.

Table 2 Scoring criteria for adverse local tissue reactions

Score	Innate inflammation (macrophages)		Adaptive inflammation (lymphocytes)		Vascularization		Necrosis
	No. of cells	Tissue % area	No. of cells	Tissue % area	No. of blood vessels	Tissue % area	Tissue % area
0	0	0	0	0	0	0	0
1	1–9	<10	1–9	<10	<10	<10	<10
2	10–50	10–50	10–50	10–50	10–50	10–25	<25
3	>50	>50	>50	>50	>50	>25	>25

Table 3 Observations of explanted Dynesys® retrieval components

Case (implantation time)	DYN 005 (2.5 years)	DYN 006 (1.9 years)	DYN 009 (2.4 years)	DYN 015 (2.2 years)	BRSP 011 (5.3 years)
Surface damages	Mild scratches	Mild scratches and abrasive wear zones	Mild scratches	Mild scratches and abrasive wear zones	Mild Scratches and abrasive wear zones
Spacer	S2	S2/B	S2/S3/S4	L S1/L S2/R S2	R 2/L1/L2/L3
Length (mm)	13.12	11.67	16.9/16.82/16.57	30.44/23.26/24.88	16.68/19.77/15.19/24.96
Angle of deformation (°)	2.03	0.2	1.47/4.34/1.73	1.32/2.32/13.6	0.59/6.46/0.52/0.25
Imprint of cord	Yes	Yes	Yes	Yes	Yes
Imprint of pedicle screw	Yes	Yes	Yes	Yes	Yes
PET cord	Fraying of fibers	Fraying of fibers	Fraying of fibers	Fraying of fibers	Fraying of fibers and fractured cord
Pedicle screws	Unremarkable	Unremarkable	Unremarkable	Unremarkable	Unremarkable

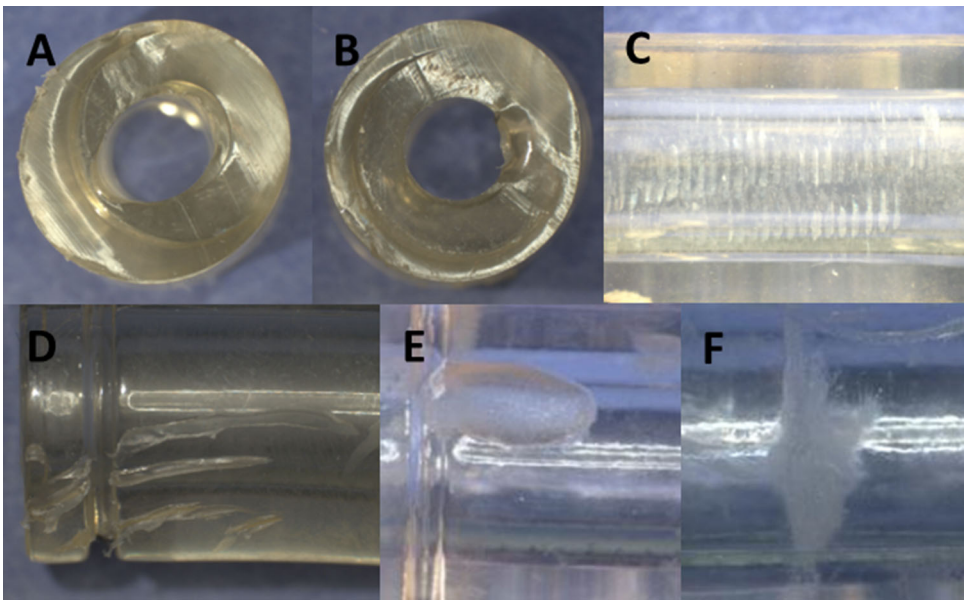

Fig. 1 Exemplary optical findings of the surface damage to the PCU spacer. **a** Pedicle screw imprint at machined end; **b** pedicle screw imprint at cut end; **c** imprints of the PET cord at the inner wall of the PCU spacer; **d**, **e** scratches and cuts on the surface of the PCU spacer; and **f** abrasive wear zone of a spacer

In all cases, some regions of the tissue were necrotic or undergoing karyorrhexis/karyolysis and loss of tissue matrix organization (Fig. 6a). Associated with these regions were areas transitioning into fibrocartilage (metaplasia), which was most prominent in tissues from patient DYN 015 with evidence of bony overgrowth at revision surgery (Fig. 6b). MicroCT images of the tissue samples also showed bone formation or heterotopic ossification in tissues from DYN 015 and BRSP 011. Vascularization was absent in the regions of necrosis and fibrocartilage formation, and in general, the amount of vascularization varied within tissues and between patient tissues (Fig. 6c).

Wear debris analysis

Wear particles were detected in three patients‘ tissues: DYN 006 (3.6 particles/mm^2, 0.11 % area of tissue occupied by wear debris); DYN 015 (6.0 particles/mm^2, 0.01 % area); and BRSP 011 (575.4 particles/mm^2, 2.63 % area) (Table 5). The particle load (particles/mm^2) was

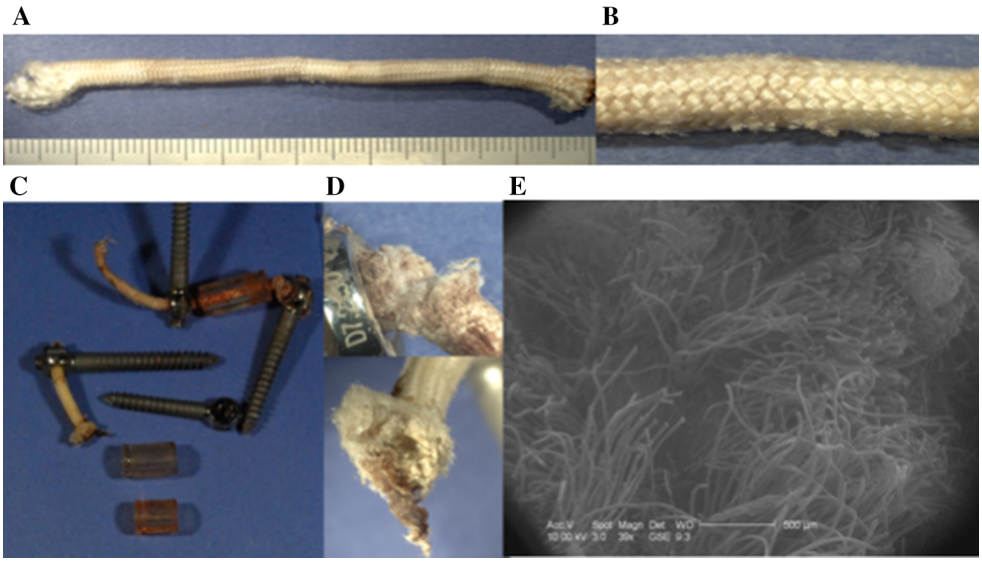

Fig. 2 Representative images of PET cord fraying and disruption from the explanted implant of patient BRSP 011. Images of PET cord fraying at **a** low magnification and **b** high magnification. **c** Disrupted left cord image, **d** higher magnifications of the disrupted cord ends and **e** SEM image of the cross section of one disrupted end

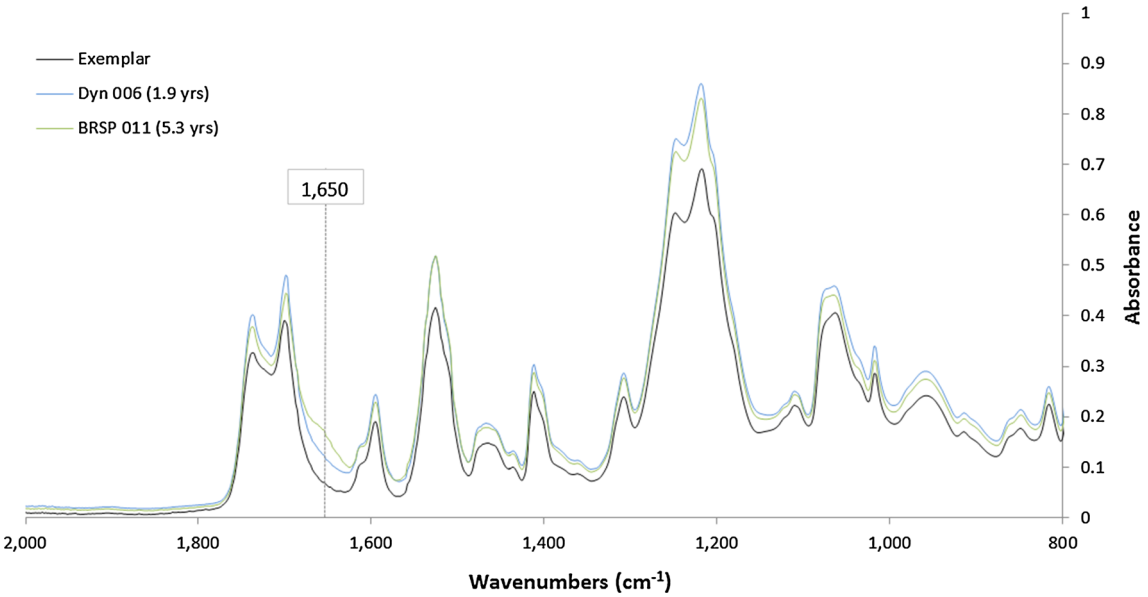

Fig. 3 Representative attenuated total reflectance Fourier transform infrared spectroscopy (ATR-FTIR) spectrums. Absorbance indicative of oxidative degradation at 1,650 cm^{-1} and an overall altered carbonyl signal was observed prominently in the longer-implanted BRSP 011 compared to other retrievals and exemplar spacers

exceptionally high for BRSP 011, which was attributed to the relatively large deformation angles and abrasive wear zones of the PCU spacers, as well as the disrupted PET cord (Table 1). The size of the particles for BRSP 011 also varied considerably in comparison to the other two patients.

Most of the particles for all three patients were within the 1–10 μm range. However, particles in the >10 μm range for case DYN 006 were much larger, ECD (33.3) and median perimeter (115.7), compared to those observed in tissues from BRSP 011 (17.2 and 68.3). Due to the increased particle size, and the absence of particles >10 μm in tissues from DYN 015, the % area of tissue occupied by particles was higher for DYN 006, despite the lower overall particle number. In all cases, the particles tended to be round and circular in shape, with a low aspect ratio.

Table 4 Histomorphology of the periprosthetic tissues

Case (implantation time)	DYN 005 (2.5 years)	DYN 006 (1.9 years)	DYN 009 (2.4 years)	DYN 015 (2.2 years)	BRSP 011 (5.3 years)
µCT	NA	NA	No bone	Bone	Bone
General tissue morphology	Well organized dense fibrous tissue	Dense fibrous tissue, more heterogeneous	Dense fibrous tissue	Dense fibrous tissue, bony overgrowth	Dense fibrous tissue, irregular morphology
Tissues	3 Tissues	3 Tissues	2 Tissues	2 Tissues	2 Tissues
Vascularization	1	1	3	2	1
No. of blood vesels	18	20	52	48	4
Macrophages	0	Isolated area in one tissue	0	1	2 Giant cells were also present in all 3 tissues
Lymphocytes	0	0	0	0	0
Necrosis	0	3	2	2	2
Fibrocartilage	One isolated area near a necrotic region		One isolated area near a necrotic region	One tissue was all fibrocartilage	One tisue contained a slender region of fibrocartilage
Bone				One tissue was 50 % bone	One tissue was 25 % bone

Mean scores are provided for each patient. *NA* not available, the tissue was processed before microCT analysis. Scoring criteria are provided in Table 2

Discussion

To evaluate the in vivo performance of Dynesys® stabilization systems, the objectives of this study were to collect implant damage information, determine the presence of wear debris and score the corresponding local tissue reactions in periprosthetic tissues. The analysis of five retrieved Dynesys® implants and periprosthetic tissues revealed similar findings for two cases (DYN 005 and 009). For these cases, the implant in vivo performance appeared to be largely unchanged with minor surface damage, reflecting the unremarkable histological appearance of the periprosthetic tissues and the lack of wear debris and inflammation. The other three cases had spacers with abrasive wear zones and tissues with either isolated inflammation and wear debris (DYN 006 and DYN 015), or in the case with gross implant damage, extensive inflammation and wear debris (BRSP 011). The size of the debris particles for BRSP 011 varied considerably in comparison to the other two patients, but most of the particles for all three patients were within the 1–10 µm range. The highest biological activity is considered to be within the <1 µm range, and decreases as the size of the particles increases [26].

Necrosis was detected in 4 of the 5 patient tissues; only tissues from DYN 005 showed no signs of necrosis, wear debris or inflammation. Transition from fibrous tissue into fibrocartilage was observed in 4 of the 5 cases, but was limited except for DYN 015. This transition may ultimately lead to heterotopic ossification, which was detected by microCT in tissues from DYN 015 and BRSP 011. An alternative explanation for heterotopic ossification or bony overgrowth of the Dynesys® implant for DYN 015 could be the use of autologous bone or bone substitute during a previous fusion surgery at the adjacent lower level. Finally, the Dynesys® implant is a dynamic stabilization system and both micro- and/or macromotion of the implant may cause metaplasia of fibrous tissue to fibrocartilage and eventually formation of heterotopic bone in the absence of inflammation (DYN 005 and DYN 009). For other orthopedic surgeries, especially joint replacements, heterotopic ossification is a well-known problem with a high incidence of 16–53 % [27] for total hip arthroplasties, and 1.4 and 15.2 % in patients with total disc replacement [28]. The 5-year results of Guyer et al. [29] showed heterotrophic ossification in 18.9 % of lumbar Charité discs.

The implant analyses also showed findings comparable with the literature for four cases DYN 005–015 with surface damage to the spacer and cord [18–20]. Abrasive surface damages were most likely due to contact of the spacer with bony structures. This was already postulated in earlier retrieval analyses [19, 20]. Results of the implant and tissue analysis of case BRSP 011 with PET cord failure and extensive PCU damage differed from the other cases.

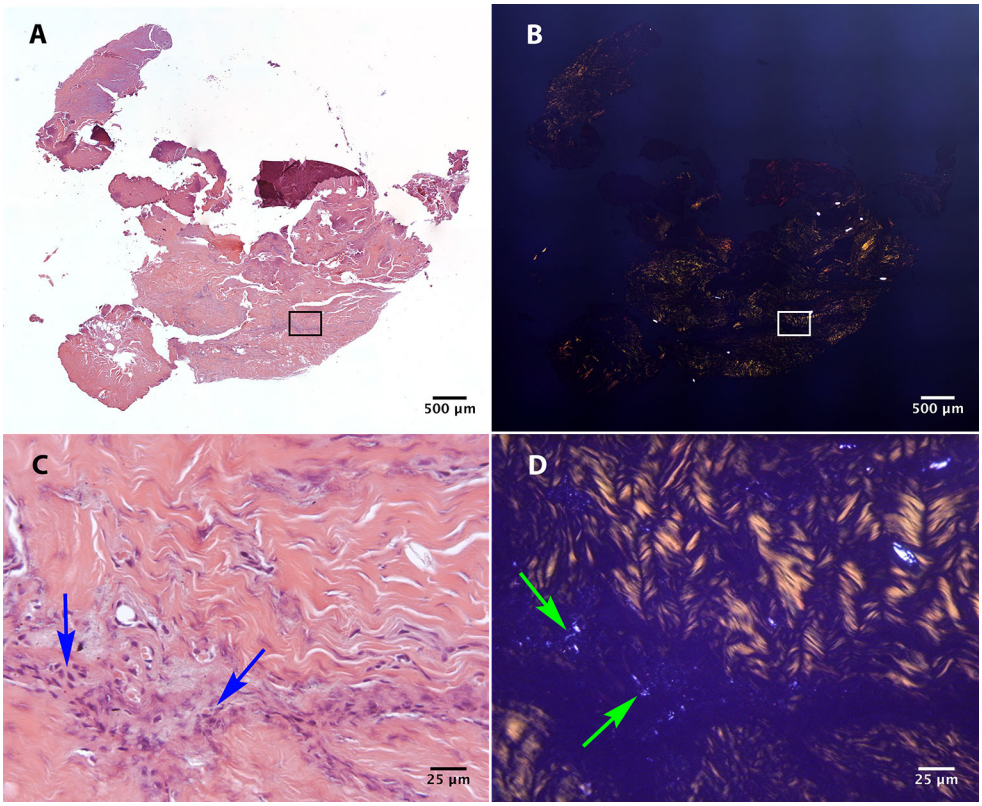

Fig. 4 Representative images from DYN 006 tissue containing infiltrating macrophages and phagocytosed debris. **a** H&E stained tissue and **b** corresponding polarized light composite **c**, **d** high magnification images of *boxed area* in **a** and **b**; *blue arrowhead* indicates macrophage infiltration and *green arrowheads* the accumulation of small wear debris. Collagen within the dense fibrous tissue appears *orange-yellow*

For this case, which was implanted for 5.3 years, the ATR-FTIR spectra showed new peaks associated with biodegradation of the PCU spacer surface. This is in agreement with the findings of Ianuzzi et al. [19], who reported that ATR-FTIR spectrum of PCU spacers implanted for longer times contained peaks associated with material degradation products. This is in contrast to the minor surface chemistry changes to the PCU spacer after implantation times of 9–19 months [18, 20].

For BRSP 011, the reasons for cord disruption and eventual problems of load distribution/transfer cannot be conclusively answered. Persisting pain and screw loosening, which was the reason for revision surgery, may be associated with chronic inflammation, which was seen in the periprosthetic tissue of this case. A possible cord rupture-related instability may have also caused the pain even though the radiography did not confirm any instability.

One limitation of this work is the low number of cases available for analysis. Nonetheless, to our knowledge, there are no published retrieval studies investigating damage and wear debris from Dynesys® implants in conjunction with the biological responses in the corresponding periprosthetic tissues. In addition, the implantation time in our cases was limited to 5.3 years and even less by taking only the intact implants into account, which may not allow conclusions on long-term biocompatibility and stability. Another limitation is that damage and chemical alterations to the devices were only assessed at the surface level, making it difficult to determine their overall impact on the mechanical properties of the entire device. Nevertheless, these factors contribute to wear debris generation, the biological response and ultimately the long-term stability and integrity of the overall implant. In addition, we were unable to detect wear particles below 0.46 µm, which are within the most biologically reactive or most inflammatory range (0.2–0.8 µm) [30]. In the two cases with less wear and surface damage (DYN 005 and 009), we did not detect wear particles, however, neither did we detect inflammatory changes within the periprosthetic tissues. Lastly, the study was only comprised of periprosthetic tissues extracted from cases requiring revision. While we have no way of precisely knowing how well-functioning Dynesys® systems wear in vivo, we are not aware of any mechanism in which these devices would generate wear and cause immune reactions in a manner substantially different from that of retrieved samples.

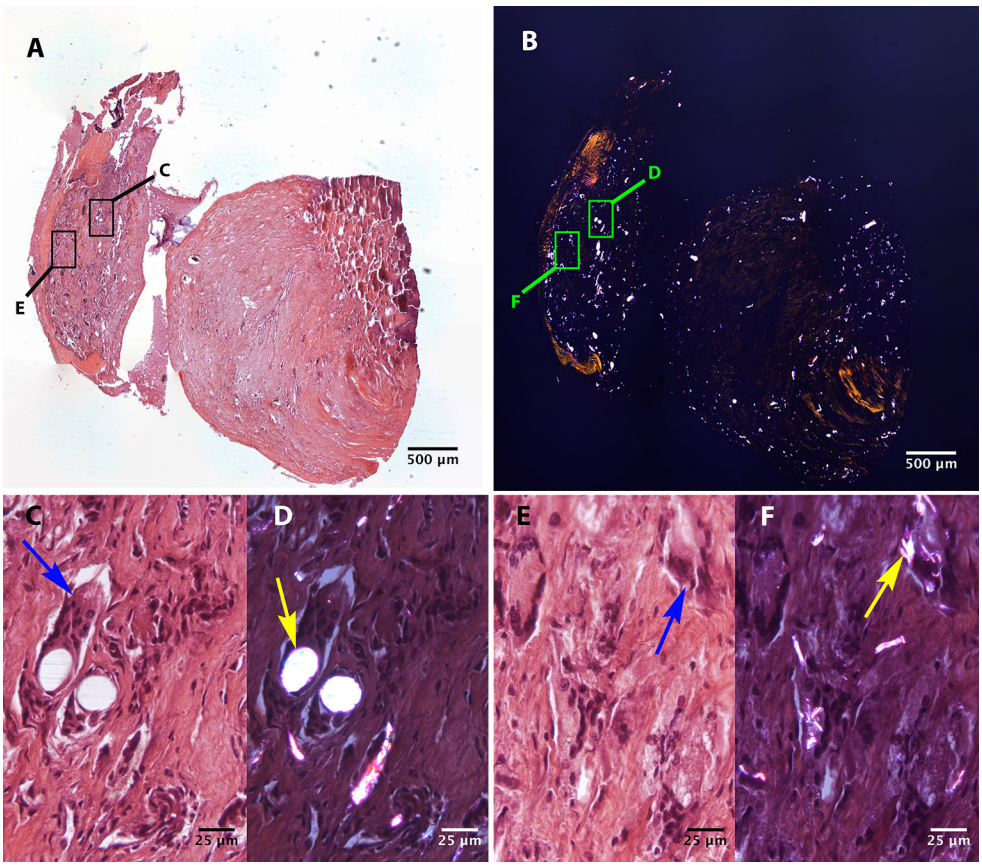

Fig. 5 Representative images from BRSP011 tissue containing large wear debris (>10 µm) and giant cells. **a** H&E stained tissue and **b** the corresponding polarized light composite. **c**, **e** high magnification images of *boxed areas* in **a**; *blue arrows* indicate giant cells. **d**, **f** corresponding images of *boxed areas* in **b**, *yellow arrows* indicates large wear debris

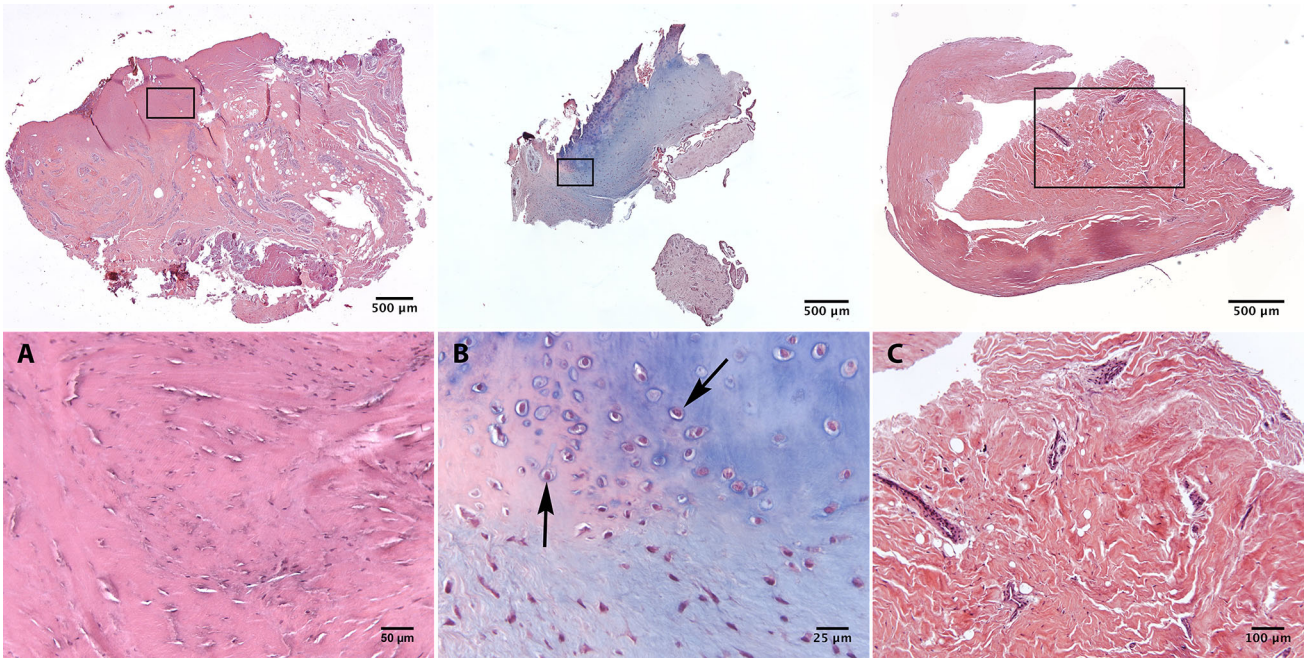

Fig. 6 Representative images showing necrosis, fibrocartilage and vascularization. Composite images of tissues taken at ×100 magnification and high magnification regions of interest. **a** a tissue with <25 % tissue necrosis (score of 2); **b** fibrocartilage and chondrocytes (*black arrows*); and **c** a tissue with <10 % vascularization (score of 1)

Table 5 Wear particle number and characteristics

Case (implantation time in years)	DYN 005 (2.5 years)	DYN 006 (1.9 years)				DYN 009 (2.4 years)	DYN 015 (2.2 years)				BRSP 011 (5.3 years)			
	All sizes	All sizes	<1 µm	1–10 µm	>10 µm	All sizes	All sizes	<1 µm	1–10 µm	>10 µm	All sizes	<1 µm	1–10 µm	>10 µm
Particles/mm^2	0	3.6	0.9	2.1	0.6	0	6.0	0.8	5.2	0	575.4	62.8	446.8	65.1
% Area of particles	0	0.11 %	0	0	0.10 %	0	0.01 %	0	0.01 %	0	2.63 %	0.00 %	0.67 %	1.96 %
ECD[a]	0	9.4 ± 14.4	0.7 ± 0.1	3.1 ± 2.0	33.3 ± 12.2	0	2.8 ± 2.0	0.8 ± 0.1	3.1 ± 1.8	0	4.9 ± 5.8	0.77 ± 0.13	3.7 ± 2.3	17.2 ± 8.7
Perimeter[a]	0	39.4 ± 66.6	3.5 ± 0.6	11.8 ± 9.4	140.6 ± 75.3	0	10.9 ± 9.8	2.6 ± 0.5	11.7 ± 8.1	0	20.1 ± 32.6	2.5 ± 0.5	14.4 ± 10.6	85.7 ± 60.5
Median perimeter		8.2	3.8	8.5	115.7	0	7.6	2.5	10.1	0	10.9	2.5	10.8	68.3
Aspect ratio (AR)[a]	0	1.9 ± 0.9	1.7 ± 0.2	2.0 ± 1.0	2.0 ± 1.1	0	1.8 ± 0.6	1.6 ± 0.3	1.8 ± 0.6	0	1.9 ± 0.8	1.6 ± 0.5	1.9 ± 0.8	2.3 ± 1.0
Roundness[a]	0	0.6 ± 0.2	0.6 ± 0.1	0.6 ± 0.2	0.6 ± 0.2	0	0.6 ± 0.2	0.7 ± 0.1	0.6 ± 0.2	0	0.6 ± 0.2	0.7 ± 0.2	0.6 ± 0.2	0.5 ± 0.2
Circularity[a]	0	0.7 ± 0.2	0.5 ± 0.2	0.8 ± 0.2	0.6 ± 0.2	0	0.8 ± 0.2	0.9 ± 0.2	0.8 ± 0.2	0	0.7 ± 0.2	0.9 ± 0.1	0.7 ± 0.2	0.5 ± 0.2

[a] Mean ± SD

Conclusions

Regarding the implant analysis and the histological findings for the four cases with an intact implant, we can assume stable conditions of Dynesys® in vivo. In the case of implant failure that is associated with cord fracture, massive inflammation due to tissue particle load can occur. Considering the small case number of this series, we would still assume that the in vivo biocompatibility of the Dynesys® stabilization system is warranted if the implant does not undergo a major failure. These assumptions can, however, only be made for the short-term follow-up. Thus, investigations of long-term retrievals will be useful in providing a larger context for the clinical implications of the observations made in this study.

Acknowledgments We thank Eual A. Phillips for his help in performing the image analyses for this paper.

IRB approval Yes.

Conflict of interest This study was supported by a grant from the NIAMS (NIH R01 AR56264). One of the authors (SMK) is an employee and shareholder of Exponent, Inc, and institutional support for SMK is received as a Principal Investigator from Smith & Nephew; Stryker Orthopaedics; Zimmer Inc; Biomet; DePuy Synthes; Medtronic; Invibio; Stelkast; Formae; Kyocera Medical; Wright Medical Technology; CeramTec; DJO; Celanese; Aesculap; SpinalMotion, Inc; and Active Implants outside of the submitted work.

References

1. Yu S-W, Yang S-C, Ma C-H, Wu C-H, Yen C-Y, Tu Y-K (2012) Comparison of Dynesys posterior stabilization and posterior lumbar interbody fusion for spinal stenosis L4L5. Acta Orthop Belg 78:230–239
2. Di Silvestre M, Lolli F, Bakaloudis G, Parisini P (2010) Dynamic stabilization for degenerative lumbar scoliosis in elderly patients. Spine (Phila Pa 1976) 35:227–234. doi:10.1097/BRS.0b013e3181bd3be6
3. Schnake KJ, Schaeren S, Jeanneret B (2006) Dynamic stabilization in addition to decompression for lumbar spinal stenosis with degenerative spondylolisthesis. Spine (Phila Pa 1976) 31:442–449. doi:10.1097/01.brs.0000200092.49001.6e
4. Schwarzenbach O, Rohrbach N, Berlemann U (2010) Segment-by-segment stabilization for degenerative disc disease: a hybrid technique. Eur Spine J 19:1010–1020. doi:10.1007/s00586-010-1282-4
5. Stoll TM, Dubois G, Schwarzenbach O (2002) The dynamic neutralization system for the spine: a multi-center study of a novel non-fusion system. Eur Spine J 11(Suppl 2):S170–S178
6. Klockner C (2010) Long-term results of the Dynesys implant. Orthopade 39:559–564. doi:10.1007/s00132-009-1585-5
7. Schaeren S, Broger I, Jeanneret B (2008) Minimum four-year follow-up of spinal stenosis with degenerative spondylolisthesis treated with decompression and dynamic stabilization. Spine 33:E636–E642. doi:10.1097/BRS.0b013e31817d2435
8. Grob D, Benini A, Junge A, Mannion AF (2005) Clinical experience with the Dynesys semirigid fixation system for the lumbar spine: surgical and patient-oriented outcome in 50 cases after an average of 2 years. Spine 30:324–331

9. Wurgler-Hauri CC, Kalbarczyk A, Wiesli M, Landolt H, Fandino J (2008) Dynamic neutralization of the lumbar spine after microsurgical decompression in acquired lumbar spinal stenosis and segmental instability. Spine (Phila Pa 1976) 33:E66–E72. doi:10.1097/BRS.0b013e31816245c0
10. Kim CH, Chung CK, Jahng TA (2011) Comparisons of outcomes after single or multilevel dynamic stabilization: effects on adjacent segment. J Spinal Disord Tech 24:60–67. doi:10.1097/BSD.0b013e3181d4eb44
11. Bothmann M, Kast E, Boldt GJ, Oberle J (2008) Dynesys fixation for lumbar spine degeneration. Neurosurg Rev 31:189–196
12. Kocak T, Cakir B, Reichel H, Mattes T (2010) Screw loosening after posterior dynamic stabilization–review of the literature. Acta Chir Orthop Traumatol Cech 77:134–139
13. Lutz JA, Otten P, Maestretti G (2012) Late infections after dynamic stabilization of the lumbar spine with Dynesys. Eur Spine J 21:2573–2579. doi:10.1007/s00586-012-2366-0
14. Ko C-C, Tsai H-W, Huang W-C, Wu J-C, Chen Y-C, Shih Y-H, Chen H-C, Wu C-L, Cheng H (2010) Screw loosening in the Dynesys stabilization system: radiographic evidence and effect on outcomes. Neurosurg 28:E10. doi:10.3171/2010.3.FOCUS1052
15. Schilling C, Kruger S, Grupp TM, Duda GN, Blomer W, Rohlmann A (2011) The effect of design parameters of dynamic pedicle screw systems on kinematics and load bearing: an in vitro study. Eur Spine J 20:297–307. doi:10.1007/s00586-010-1620-6
16. Gedet P, Haschtmann D, Thistlethwaite PA, Ferguson SJ (2009) Comparative biomechanical investigation of a modular dynamic lumbar stabilization system and the Dynesys system. Eur Spine J 18:1504–1511. doi:10.1007/s00586-009-1077-7
17. Schmoelz W, Huber JF, Nydegger T, Dipl I, Claes L, Wilke HJ (2003) Dynamic stabilization of the lumbar spine and its effects on adjacent segments: an in vitro experiment. J Spinal Disord Tech 16:418–423
18. Kurtz SM, MacDonald D, Ianuzzi A, van Ooij A, Isaza J, Ross ER, Regan J (2009) The natural history of polyethylene oxidation in total disc replacement. Spine (Phila Pa 1976) 34:2369–2377. doi:10.1097/BRS.0b013e3181b20230
19. Ianuzzi A, Kurtz SM, Kane W, Shah P, Siskey R, van Ooij A, Bindal R, Ross R, Lanman T, Buttner-Janz K, Isaza J (2010) In vivo deformation, surface damage, and biostability of retrieved Dynesys systems. Spine 35:E1310–E1316. doi:10.1097/BRS.0b013e3181d6f84f
20. Shen M, Zhang K, Koettig P, Welch WC, Dawson JM (2011) In vivo biostability of polymeric spine implants: retrieval analyses from a United States investigational device exemption study. Eur Spine J 20:1837–1849. doi:10.1007/s00586-011-1812-8
21. Christenson EM, Anderson JM, Hiltner A (2004) Oxidative mechanisms of poly(carbonate urethane) and poly(ether urethane) biodegradation: in vivo and in vitro correlations. J Biomed Mater Res A 70:245–255. doi:10.1002/jbm.a.30067
22. Grammatopoulos G, Pandit H, Kamali A, Maggiani F, Glyn-Jones S, Gill HS, Murray DW, Athanasou N (2013) The correlation of wear with histological features after failed hip resurfacing arthroplasty. J Bone Joint Surg Am 95:e81. doi:10.2106/JBJS.L.00775
23. Veruva SY, Lanman TH, Isaza JE, Macdonald DW, Kurtz SM, Steinbeck MJ (2014) UHMWPE wear debris and tissue reactions are reduced for contemporary designs of lumbar total disc replacements. Clin Orthop Relat Res (in press)
24. Baxter RM, Ianuzzi A, Freeman TA, Kurtz SM, Steinbeck MJ (2010) Distinct immunohistomorphologic changes in periprosthetic hip tissues from historical and highly crosslinked UHMWPE implant retrievals. J Biomed Mater Res A 95:68–78. doi:10.1002/jbm.a.32813
25. Cipriani E, Bracco P, Kurtz SM, Costa L, Zanetti M (2013) In-vivo degradation of poly(carbonate-urethane) based spine implants. Polym Degrad Stab 98:1225–1235. doi:10.1016/j.polymdegradstab.2013.03.005
26. Fisher J, Bell J, Barbour PS, Tipper JL, Matthews JB, Besong AA, Stone MH, Ingham E (2001) A novel method for the prediction of functional biological activity of polyethylene wear debris. Proc Inst Mech Eng H 215:127–132
27. Vanden Bossche L, Vanderstraeten G (2005) Heterotopic ossification: a review. J Rehabil Med 37:129–136. doi:10.1080/16501970510027628
28. McAfee PC, Cunningham BW, Devine J, Williams E, Yu-Yahiro J (2003) Classification of heterotopic ossification (HO) in artificial disk replacement. J Spinal Disord Tech 16:384–389
29. Guyer RD, McAfee PC, Banco RJ, Bitan FD, Cappuccino A, Geisler FH, Hochschuler SH, Holt RT, Jenis LG, Majd ME, Regan JJ, Tromanhauser SG, Wong DC, Blumenthal SL (2009) Prospective, randomized, multicenter Food and Drug Administration investigational device exemption study of lumbar total disc replacement with the CHARITE artificial disc versus lumbar fusion: five-year follow-up. Spine J 9:374–386. doi:10.1016/j.spinee.2008.08.007
30. Ingham E, Fisher J (2000) Biological reactions to wear debris in total joint replacement. Proc Inst Mech Eng H 214:21–37